Power-Efficient Electron Emitters for Electron Ionization in Spaceborne Mass Spectrometers

Rico Fausch
Physics Institute, University of Bern, Sidlerstrasse 5, 3012 Bern Switzerland
rico.fausch@unibe.ch

Martina Föhn
Physics Institute, University of Bern, Sidlerstrasse 5, 3012 Bern Switzerland
m.foehn93@gmail.com

Lukas Hofer
Physics Institute, University of Bern, Sidlerstrasse 5, 3012 Bern Switzerland
lukas.hofer@gmail.com

Stefan Meyer
Physics Institute, University of Bern, Sidlerstrasse 5, 3012 Bern Switzerland
stefm@gmx.ch

Peter Wahlström
Physics Institute, University of Bern, Sidlerstrasse 5, 3012 Bern Switzerland
peter.wahlstroem@hotmail.ch

Samuel Stefan Wyler
Physics Institute, University of Bern, Sidlerstrasse 5, 3012 Bern Switzerland
samuel.wyler@unibe.ch

Peter Wurz
Physics Institute, University of Bern, Sidlerstrasse 5, 3012 Bern Switzerland
peter.wurz@unibe.ch

2024 IEEE Aerospace Conference | 979-8-3503-0462-6/24/$31.00 ©2024 IEEE | DOI: 10.1109/AERO58975.2024.10521278

Abstract—**Robust cathodes are used as electron emitters to ionize neutral atoms and molecules by electron ionization in spaceborne mass spectrometers. These instruments require an electron emission current of about 50 to 1000 µA from the emitters. The emitters must be power-efficient, robust with respect to handling, and withstand launch into space. In addition, the lifetime driven by the mission design influences the selection of the cathode. The required lifetime is a result of the sum of the nominal scientific operation time in space, the time operated during both pre-launch and post-launch commissioning, potential mission extension if applicable, and margin. For example, a simple lunar landing mission such as the Neutral Gas Mass Spectrometer (NGMS) on board the Luna 27 mission requires a nominal total lifetime of the cathodes of about 4,000 hours. In contrast, the team specified 10,000 hours as a requirement for the Neutral and Ion Mass spectrometer (NIM) on board ESA's large-class Jupiter's Icy Moon Explorer (JUICE) mission. Here, we present a study to identify the flight cathodes for NGMS/Luna-Resurs, NIM/JUICE, and their successor instruments MANIaC and its Neutral Density Gauge (NDG) on board Comet Interceptor. The analysis includes a detailed survey of concepts presented as review with subsequent laboratory investigation of promising candidates. The realized concepts included prototypes with, on one hand, innovative concepts relying on field effect and secondary electron emission namely two types of Carbon Nano-tubes (CNTs) and an UV-LED triggered microchannel plates (MCPs), overcoming the microtips Spindt type cathodes. On the other hand, ten types of thermionic emitters are analyzed with materials including BaO, LaB_6, WRe, WTh, and Y_2O_3. The tests conducted in this framework included laboratory testing with respect to the mentioned requirements especially focusing on both normal and accelerated life testing and advanced surface analysis (SEM with BSE, SE, and EDX). We established a simple metric to compare the results of these tests. In addition to the empirically derived parameters for such a metric, the current market situation, i.e., the availability of the cathodes, strongly influenced the selection of flight cathodes. For example, due to a shift in technology of consumer electronics for (cathode-ray tube) televisions, several best-of-class oxide cathodes suddenly became unavailable. In addition, potentially suitable cathodes used for calibration of the ROSINA instrument on board the ROSETTA mission became unavailable as well. Among the remaining candidates, we selected an yttrium-oxide coated thermionic disc cathode for NGMS consuming about 1.6 W satisfying its lifetime requirement. For NIM, the same cathode was further enhanced to achieve a nominal power consumption of about 1.1 W, whilst increasing their lifetime to comply with the mission requirements. Recently, we successfully commissioned one of the cathodes on board the flight instrument of NIM during the Near-Earth Commissioning Phase (NECP) shortly after launch, attesting the quality of the analysis presented in this paper. This success enables NIM to analyze the neutral exospheres of Jupiter's icy moons Europa, Ganymede, and Callisto and potentially providing insights on their subsurface oceans.**

TABLE OF CONTENTS

979-8-3503-0462-6/24/$31.00 ©2024 IEEE

1. INTRODUCTION

Durable cathodes serve as electron emitters in spaceborne mass spectrometers, playing a crucial role in ionizing neutral atoms and molecules through electron ionization elementary for analysis of neutral gas.

Electron ionization requires an electron source consisting of three main elements namely release of electrons from condensed matter into in free vacuum, electron optics for acceleration, transport and beam shaping, and the very ionization process itself.

Electrons colliding with the chemical species under analysis, i.e., neutral atoms and molecules, convert neutral species into mostly positive ions by ejecting one or more electrons from the neutral species. Although the onset ionization energy of single charged both neutral atoms and molecules is in the order of some eV to 25 eV for He, a maximum of the ionization cross section σ of species is observable at about 70 eV–100 eV [1]. This electron energy optimizes the achievable total ion current I^+ of the ion source in relation to the electron current I_e−:

$$I^+ = \beta n_0 \sigma d {I_e}^{-s} \tag{1}$$

where β is the ionization probability, n_0 the gas number density inside the ionization region, the storage factor *s*, and *d* the total derivative of the electron's trajectory. The electron current is referred to as anode current, sometimes called (electron) emission current. The distance is in the order of cm. For reference, at a pressure of 10^{-4} mbar $= 10^{-2}$ Pa that equals $n_0 \approx 10^{12}$ cm^{-3}, the mean free path is about 1 m, which can be assumed as free vacuum. An electron impact energy 70 eV represents a reasonable trade-off between efficient electron ionization and fragmentation caused by the process. Relevant ionization potentials, cross sections, and fragmentation patterns are well described in the NIST library [2]. Deviating from this commonly used energy had been shown to be complicated. For lower (or higher) energies, fragmentation patterns needed to be recalibrated resulting in extensive laboratory campaigns as performed, for example, for the ROSINA/ROSETTA instrument suite [3], [4].

Electron optics moderates the ionization energy and defines the ionization region. For time-of-flight (TOF) mass spectrometers, in a simple assumption, electron ionization would be optimal to happen in a two-dimensional circle, with its normal vector pointing into the acceleration direction of the mass analyzer, i.e., the ion-optical axis. Statistically, in a modern ion-optical system with a transmission of 1, this would cause a complete illumination of the detector, by the mass analyzer. This is especially relevant for compact detectors using multi-channel plates. However, the sensitivity of TOF instruments is considerably increased by introducing ion-storage sources. Ideally, they require a collimated beam of electrons. The negative space charge of the electron beam creates a potential well, which attracts the cations causing them to orbit around the beam. The potential well created by the charges increases the duration of staying inside the ion source. Hence, the storage factor *s* in Equation (1) equals $s = 1$ if there is no storage, $s = 2.75$ if there is nominal storage, and $s = 1.75$ if the ion source operates in saturation mode due to increased space charge [5]. References [3], [5]–[8] discuss the design of ion sources and their regimes in detail. To make use of ion storage, the ion source requires a direct current from the electron emitter.

Electron optics directly relates to the extraction of electrons from solids. In plasma physics, the Child-Langmuir law [9], [10] describes the limit of the current that can be extracted from a surface, as limited by space charge. Surface-near electrons create space charge repelling further electrons from being extracted. Applying a voltage *V* to the surface, for example, in a diode configuration, i.e., a plate capacitor, the maximum anode current density *j* in A/cm^2 follows the relation:

$$j = \frac{{I_e}^-}{A} = \frac{4\sqrt{2}}{9}\epsilon_0\sqrt{\frac{e}{m}}\frac{V^{3/2}}{d^2} \tag{2}$$

where ϵ_0 is the free space permittivity, *e* the elementary charge, *m* the mass of the electron, *d* the anode–cathode gap, *A* the area of interest. This voltage is referred to as anode voltage or extraction voltage. In simplified form, the above equation reads:

$$j = \alpha \cdot V^k \tag{3}$$

where α (in A cm^{-2} V^{-k}) and k (unitless) are the fit parameters.

In principle, *V* might be increased to high values with a subsequent deceleration of the electrons to achieve the required total integral acceleration voltage of 70 V. However, the theory of electron optics shows that the deceleration of an electron beam also leads to defocusing of the beam. One or more Einzel lenses, sometimes including a Wehnelt cylinder, focus the beam inside the electron emitters. The LACE instrument on board Apollo used an ionization energy of either 70 eV or a sequence of 70, 27, 20, and 18 eV altering subsequently in a scanning mode [11]. Scanning through the ionization energy provided additional information for identification of complex species via their energy dependent fragmentation patterns. This is useful for instruments on stationary landers or rovers in a quasi-static atmosphere. During descent, flybys, or when orbiting, scanning results in a loss of spatial information [12]. Hence, to achieve the

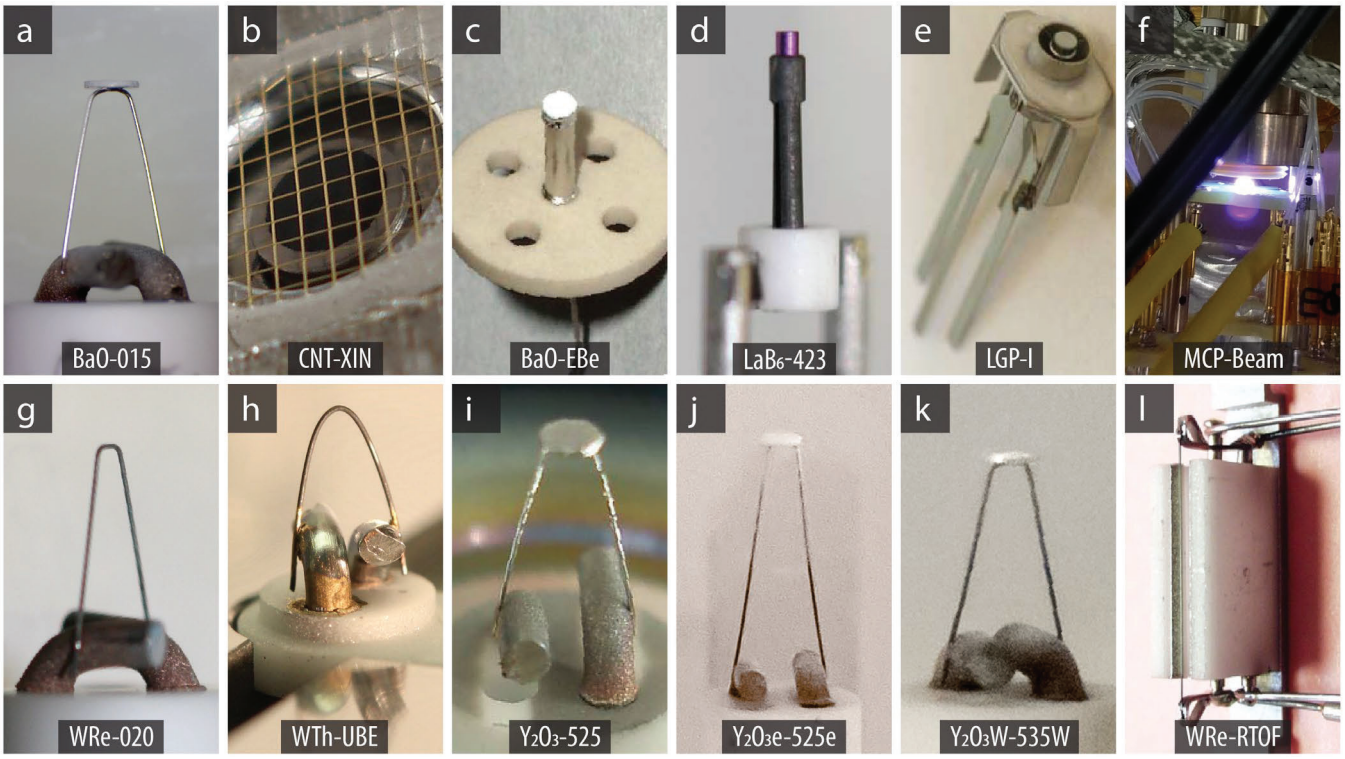

Figure 1. We tested 12 candidate electron emitters to select a suitable type for NGMS / Luna 27 (i), NIM / PEP / JUICE (j), and MANIaC / Comet Interceptor (j).

desired anode current of about $I_{e^-} = 10$ to 1000 µA, as typically required by mass spectrometers, the cathode must be able to deliver a suitable current density according to their emitting geometry, i.e., surface A.

2. Previously Used Cathodes

In the early days of space instrumentation, thermionic emitters served as robust cathodes. Inside condensed matter, an electrostatic barrier prevents electrons from leaving the material. In hot emitters, joule heating modifies the Fermi energy distribution until a reasonable number of electrons have enough energy to overcome the material specific work function Φ and eventually emit into free vacuum. The Richardson equation describes the anode current density j

$$j = A_G T^2 e^{\frac{-\Phi}{k_B T}} \quad (4)$$

where A_G is a material specific parameter, here referred to as Richardson constant, T the cathode's absolute temperature, and k_B the Boltzmann constant [13], [14]. Consequently, the geometry of the emitter and its heating current, referred to as the cathode current I_c, determine the effectively available anode current and thus the ion current.

Size, weight, and power consumption of cathodes are mainly driven by the emission temperature of the cathode and the capability to thermally isolate the emitting region while maintaining a high electrical conductivity to dissipate joule heating where needed. Several variations of both geometry (hairpin, single wire, coil, etc.), and alloys have been used to both increase the emitting area to overcome current density limitations and to minimize the power consumption of the hot emitters.

Table 1 shows both an overview and references of the materials and ionization parameters used where available in the literature (private communication omitted). In brief, most filaments contain tungsten in geometries of straight wires or bands, coils, and hairpins. The work function of tungsten can be lowered considerably by alloying it with various materials (see reference [15]–[18]). A rhenium alloy (about 3%), for example, makes the wires more ductile. This was already well known at the time of the Apollo missions, with which the LACE mass spectrometer flew. It contained two redundant tungsten with 1% rhenium (WRe1) filaments [11]. A benefit of these tungsten filaments is their robustness. They are immune to air exposure, cathode poisoning, outgassing, temperature stress, and their geometries lead to very low mass, helpful to survive vibration and shock testing for space launch. The typical wire diameter is in the order of 100 µm.

The work function can also be decreased by alloying the material with 1 to 15 % thorium [19] as used for MENCA on board the Mars Orbiter Mission. As thorium is a radioactive alpha emitter, handling the cathode requires increased safety concepts, complicating the testing and commissioning phase.

Accurately controlling the cathode current improves lifetime. Equation (1) implies a high sensitivity to temperature. Depending on the cathode, an increase of a cathode

Table 1. Overview of flight cathodes. This table supplements the data in reference [20], specifically focusing on information pertinent to electron ionization, where found (N/A indicated otherwise). *: Potential converted into energy. TBD: to be defined. ‡: this study.

Mission target	Mission	Instrument	Type	Year	Cathode parameters	Ionization parameters	Ref.
Mercury	BepiColombo	STROFIO	TOF	2018–	BaO-Ebe: E-beam impregnated cathode	70 eV nominal, 0 – 1000 µA	[21]–[23], ‡
Venus	Venera 11–12	Mass spectrometer	Quadrupole	1969–1982	N/A	40 eV*, 400 µA	[24]
	Pioneer Venus Orbiter	ONMS	Quadrupole	1978–1992	N/A	27, 70 eV	[25], [26]
Earth	Dellingr	INMS	TOF	2018	Carbon coated cathode	N/A	[27]–[29]
	CHESS	CubeSatTOF	TOF	2027	2 redundant Y_2O_3e-525e	70 eV nominal, 0 – 1000 µA	[30], ‡
Moon	Apollo 17	LACE	Magnetic	1972–1972	2 redundant WRe1	70 eV const. or scanning 70, 27, 20, 18 eV	[11]
	LADEE	NMS	Quadrupole	2013–2014	127 µm, 6-coil WRe3	20 – 400 µA	[31]
	Peregrine Mission One / CLPS	PTIMS	Ion trap	2024	Heated wire filament	N/A	[32]
	VIPER / CLPS	MSolo	Quadrupole	TBD	crossbeam (XB) ionization source	N/A	[33]
	Luna 27 / TBD	NGMS	TOF	TBD	2 redundant Y_2O_3-525, AC supply	70 eV nominal, 0 – 1000 µA	‡
Mars	Viking 1 Viking 2	GCMS	Magnetic	1976–1982 1976–1980	2 redundant, u-shaped filaments	45, 70	[34], [35]
	Phoenix	TEGA	Magnetic	2008	W	90, 37, 27, 23 eV; 25 µA, 200 µA; 1 W	[36]
	Mars Science Laboratory	QMS	Quadrupole	2012–	WRe3 wire operating at about 2 V and 2 A (about 4 Watt)	70 eV, 10 – 400 µA, nom. 20 or 200 µA	[37]
	MAVEN	NGIMS	Quadrupole	2014–	127 µm, 6-coil WRe3	70 eV, 20 – 400 µA, nom. 50 or 250 µA	[38]
	Mars Orbiter Mission	MENCA	Quadrupole	2014–2022	2 redundant Th coated Ir substrate filament	70 eV	[19]
	Rosalind Franklin / TBD	MOMA	Ion trap	2028–	2 redundant 76 µm, WRe3 filaments, AC supply	70 eV 10 – 100 µA	[39], [40]
Jupiter	Galileo	GPMS	Quadrupole	1995–1995	2 redundant filaments	15, 25, 75 eV	[41]
	JUICE	NIM	TOF	2030–	2 redundant Y_2O_3e-525e, AC supply	70 eV nominal, 0 – 1000 µA	[7], [42], ‡
	Europa Clipper	MASPEX	TOF	2030–	WRe3	N/A	[43]
Saturn	Cassini	INMS	Quadrupole	2004–2017	2 redundant 76 µm coiled WRe3	25, 70 eV 40 µA	[44]
Titan (moon)	Cassini-Huygens	GCMS	Quadrupole	2005	76 µm wire, WRe3, 1 W	25, 70 eV 80 µA typical	[45]
Comet - 67P	Rosetta	DFMS	Magnetic	2014–2016	2 redundant WRe3	10 – 90 eV 2, 20, 200 µA	[3]
	Rosetta	RTOF	TOF	2014–2016	2 redundant WRe3 bands, about 2 W	70 eV typical, 30 – 150 V, 20 – 200 µA	[3]
	Rosetta	COSAC	TOF	2014–2016	3 redundant 25 µm Y wires with 75 µm Y_2O_3 coating, 1.5 W	N/A	[46]–[48]
	Rosetta	Ptolemy	Ion trap	2014–2016	3 x 2 x (40 x 40) nanotips array	N/A	[49]
Comet - unknown	Comet Interceptor	MANIaC	TOF	2029–	2 redundant Y_2O_3e-525e	70 eV nominal, 0 – 1000 µA	‡

temperature of already 100 °C decreases the lifetime by a factor of 10 [50].

There is a tradeoff between lifetime, power consumption, and scientific performance. The cathode in the magnetic sector type TEGA instrument on board Phoenix employed a tungsten filament providing anode currents of 25 µA or 200 µA. Hoffman et al. [36] reported an increase of the dynamic range by a factor of 8, implying no ion storage capabilities, as expected for this type of mass analyzers. The filament including controller was claimed to consume 1 W, which is exceptionally energy efficient especially when regarding the expected nominal lifetime of the mission of 90 Martian sols ground time (approximately 2,200 hours, total ground time of the platform, no information of the operation time found), which was finally extended to 157 sols (approximately 3,870 hours). In contrast, QMS / MSL used a WRe3 wire filament operating at 2 V and 2 A and thus consuming about 4 W [37]. Whereas hairpin filaments are very power efficient but are known to have an operational lifetime in the order of hundreds of hours, wire filaments or even more complex geometries may achieve lifetimes of two or more decades more (see reference [51]). Therefore, effective power consumption is strongly influenced by the mission's lifetime requirements. Typical expected lifetimes of cathodes are in the order of 1000 hours for a mission to the Moon, as foreseen by NGMS / Luna 27 [52]. However, required lifetimes can easily reach 10,000 hours for deep space missions such as, for example, NIM / PEP / JUICE [7] or NMS / Interstellar Probe [25]. Such missions include a descent pre-launch commissioning phase, calibration, post-launch (near-Earth) commissioning, nominal operation, and potential mission extension(s). In addition to carefully controlling the temperature of the filament, redundancy of the cathode and other components increases the overall probability of failure free operation.

The use of tungsten type cathodes in space instrumentation is in stark contrast to parallel developments of industrial products minimizing the power consumption while increasing lifetimes. Driven by the consumer market for cathode ray tube (CRT) television (e.g., references [53], [54]), the initially used impregnated cathodes were widely replaced by oxide and cermet cathodes. Especially oxide cathodes drew attention with the introduction of rare-earth element doping in the oxide layer and the introduction of the 'Oxide Plus' cathode produced by L.G. Philips Displays [16], [55]. This iconic cathode showed about 20,000 hours nominal operational lifetime at a power consumption of about 0.65 W [56]. With the shift in technology in the consumer market away from CRT television in about 2007, these cathodes became rare and later even unavailable [17].

Applying high fields to the surface increases the anode current leading to Schottky emission and, for even higher fields, to Fowler–Nordheim (FN) when electron tunneling dominates the anode current. Carbon nanotubes and field emitter arrays [57], [58] show remarkably low power consumption, as no heating is needed in this regime and basically the only consumer is the high voltage power supply providing the necessary field strengths. The resulting narrow energy distribution at a low temperature enabled measurements of low energetic particles inside ROSETTA's comet pressure sensor (COPS) by employing a Spindt type microtips cathode with a resistive layer serving as arc generation protection, which increased the lifetime [3], [59]–[61]. The manufacturer specified a lifetime of about 20,000 hours. These emitters were rigorously tested [62] and flight qualified. The 32 x 32 pixels tip array occupied an area of 14 x 14 mm^2 and the microtips were vertically grouped into eight either sequentially or jointly operational units. Each of these groups could emit 1 mA at 70 V extraction voltage. Thanks to these unique cathodes, the total power consumption of the ram gauge of COPS was less than 0.7 W. These microtips were later used in related calibration facilities [63] but became unavailable as well.

Microchannel plates create an avalanche of electrons to convert single ions or photons into a charge cloud with a typical gain of 10^5 to 10^6 per event. Given the typical peak width of about 100 to 500 ps, a single event results in a current of 100 µA, comparable to the required anode currents. Schiedt and Weinkauf [64] used such a concept as electron source, but the technical readiness level was low, and the electron source was commercially unavailable. Another group realized an MCP-based electron source with electron anode currents of up to 10 µA in continuous emission mode and 10 mA in pulsed emission mode [65], which found application in a portable TOF-MS [66].

The product lifecycles of cathodes cause engineering teams developing mass spectrometers to investigate novel cathodes for almost every upcoming mission. Therefore, we analyzed the market multiple times and developed cathodes both in house and in collaboration with industry, always driven by the requirement to fly cathodes consuming around 1 W while achieving the requested lifetimes. Here, we discuss the cathodes and relevant selection considerations related to P-BACE / MEAP [67], STROFIO / BepiColombo [22], NGMS / Luna 27 [52], [68], NIM / PEP / JUICE [7], CubeSatTOF / CHESS [30], and SHU and NDG of MANIaC / Comet Interceptor [69].

3. Material and Methods

After developing the ROSINA / ROSETTA payload and given the shortage of the Spindt cathode, we considered many cathodes for spaceflight. Table 2 shows an overview of the cathodes considered for various missions in context of time. The P-BACE instrument on board MEAP is a miniaturization of the RTOF / ROSINA / ROSETTA instrument from about 1 m length to 30 cm length and served as design baseline for all following instruments, except for STROFIO / BepiColombo and CubeSatTOF / CHESS, the latter is a further miniaturization to 10 cm. Table 3 provides a detailed overview of the cathodes, their types, and names. For P-BACE, the LaB_6-423 cathode was used, as the mission

needed to fly within 6 months of development time. Its prototype was operated with this cathode despite consuming close to 4 W (see also Figure 5). The cathode operated stable both in the laboratory and during flight.

Table 2. Timeline of mission and cathode development discussed in this study.

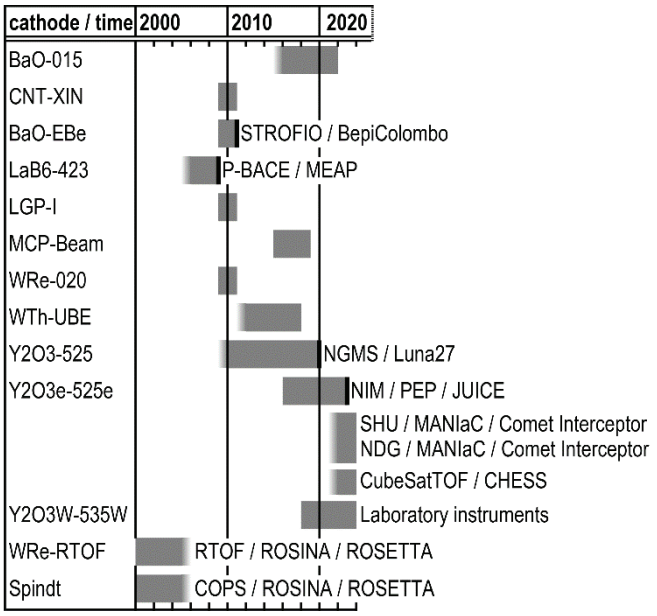

STROFIO / BepiColombo required a power consumption below 2 W for an anode current of 1 µA and a nominal lifetime of about 1 year. Hence, LGP-I, BaO-EBe, WRe-020, and Y_2O_3-525 were considered as thermionic emitters (see also Figure 1). These cathodes were tested in a versatile setup with diode configuration (Figure 2, panel a, b). The cathodes were screened for suitability, which includes testing of the operation characteristics. The best cathodes were tested in a batch to verify the selection (Figure 2, panel c). Additionally, a second batch was tested to identify the very flight cathode, by carefully analyzing the surface with secondary electron microscopy upon a short functional verification during the commissioning (see reference [23]).

At that time, carbon nanotubes (CNTs) became increasingly available. As the cold emitters of ROSINA were promising, we tested CNT-XIN, which we assembled in house and tested in a dedicated setup (Figure 1, panel b). We used a coarse extraction grid with a geometrical transmission factor of 0.85 to establish the field strength necessary for electron extraction.

For NGMS / Luna 27 [70], [71], and later NIM / PEP / JUICE [7], [42], [72], we surveyed the market again. BaO-015, WTh-UBE, MCP-Beam, and Y_2O_3-525 were considered. The procedure was like the one indicated before. Various versions of the WTh-UBE cathodes were fabricated, i.e., we experimented with the thickness of the wire of this hairpin filament (see Figure 1, panel h).

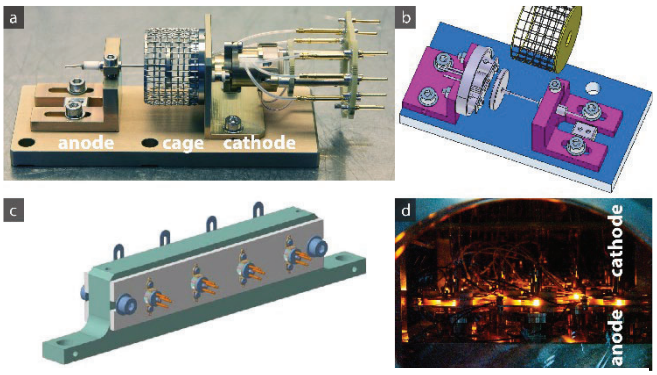

Figure 2. The multi-purpose diode setup was used for testing the MCP-Beam (a), LGP-I (b), and most others listed in Table 3. The BaO-EBe cathode for STROFIO required a different setup for batch testing (c). A setup mocking the NIM ion source was used for testing the NIM filaments in a batch of 20 (d).

The MCP-Beam setup required a customized design. Figure 3, panel a, shows the concept. A trigger signal causes the UV-LED to emit photons, which are then transported via optical fiber to a diffusor illuminating the complete surface of the first microchannel plate (MCP). Ultraviolet light increases the detection efficiency of the MCPs as compared to VIS/IR. The MCPs are operated with a high voltage (HV) power supply, in the order of 2 kV. Additional low voltages (LV) provided focusing of the beam. Figure 3, panel b, shows the related SIMION simulation (a commercial software package for simulating ion- and electron-optical systems).

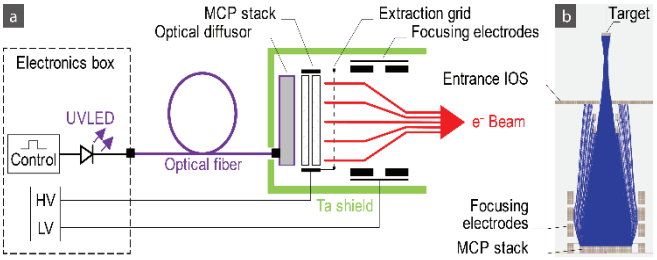

Figure 3. Concept of the MPC-Beam emitter. A LED emits light in UV at the desired instance triggering secondary electron emission in the MCP (a). An electron-optical system supplied by both high and low voltages (HV, LV) focuses the emitted electrons to form an electron beam (b).

Initially, the selection criteria were dominated by power consumption and lifetime, which can be derived from data sheets and testing. For the missions following STROFIO / BepiColombo, we added requirements to better account for the handling, especially with respect to radioactivity and venting cycles, i.e., immunity (or close to) towards air exposure upon operation. Both requirements became Go / No-Go criteria.

Table 3. Overview of the assessed cathodes in a given setup (X). Column # refers to the label indicated in Figure 1. Details are provided in the text and details of the manufacturer in Appendix A. *: on CB-104 base. The availability is reassessed on October 1, 2023 (†), where ● refers to available and ○ to end of product life. ○/● Technology remains available in principle, but no suitable cathodes are available. ‡: for reference, not part of this study.

#	Designator	Emission type	Description	Manufacturer	Tested in setup / model				Status now †
					Diode, triode	Life test	Prototype, EM, EQM	Flight model	
a	BaO-015	Thermionic	Barium Oxide Coated Disc Cathodes (ES-015*)	Kimball Physics Inc.	X	X	X		●
b	CNT-XIN	Field	Carbon nanotube diameter 2.5 mm (XTC-D01-SSC-C2.5x2.5)	Xintek Inc.	X				○/●
c	BaO-EBe	Thermionic	BaO impregnated cathode	E-Beam Inc.	X	X		STROFIO / Bepi-Colombo	○
d	LaB_6-423	Thermionic	Lanthanum Hexaboride Single Crystal Cathodes (ES-423*)	Kimball Physics Inc.	X	X	X	P-BACE / MEAP	●
e	LGP-I	Thermionic	LG-Philips Impregnated cathode	LG-Philips	X				○
f	MCP-Beam	Secondary electron	Microchannel plates triggered with UV-LED (LZ1-00UV00 or LEUVA66B00HF00)	Photonis USA Inc., LED Engin Inc., LG Innotek Co. Ltd.	X				○/●
g	WRe-020	Thermionic	Tungsten rhenium (3 %) hairpin (ES-020*)	Kimball Physics Inc.	X				○
h	WTh-UBE	Thermionic	Tungsten (85%) thorium (15 %) hairpin*	University of Bern	X		X		●
i	Y_2O_3-525	Thermionic	Yttria coated iridium disc cathode (ES-525*)	Kimball Physics Inc.	X	X	X	NGMS / Luna 27	○
j	Y_2O_3e-525e	Thermionic	Customized Y_2O_3-525 cathode with enhanced coating (ES-525B*)	Kimball Physics Inc.	X	X	X	NIM / JUICE, MANIaC / Comet Interceptor, CubeSatTOF / CHESS	●
k	Y_2O_3W-535W	Thermionic	Yttria coated iridium disc cathodes, tungsten wire (ES-535W*)	Kimball Physics Inc.			X		●
l	WRe-RTOF‡	Thermionic	Tungsten rhenium	University of Bern	X	X	X	RTOF / ROSETTA	●

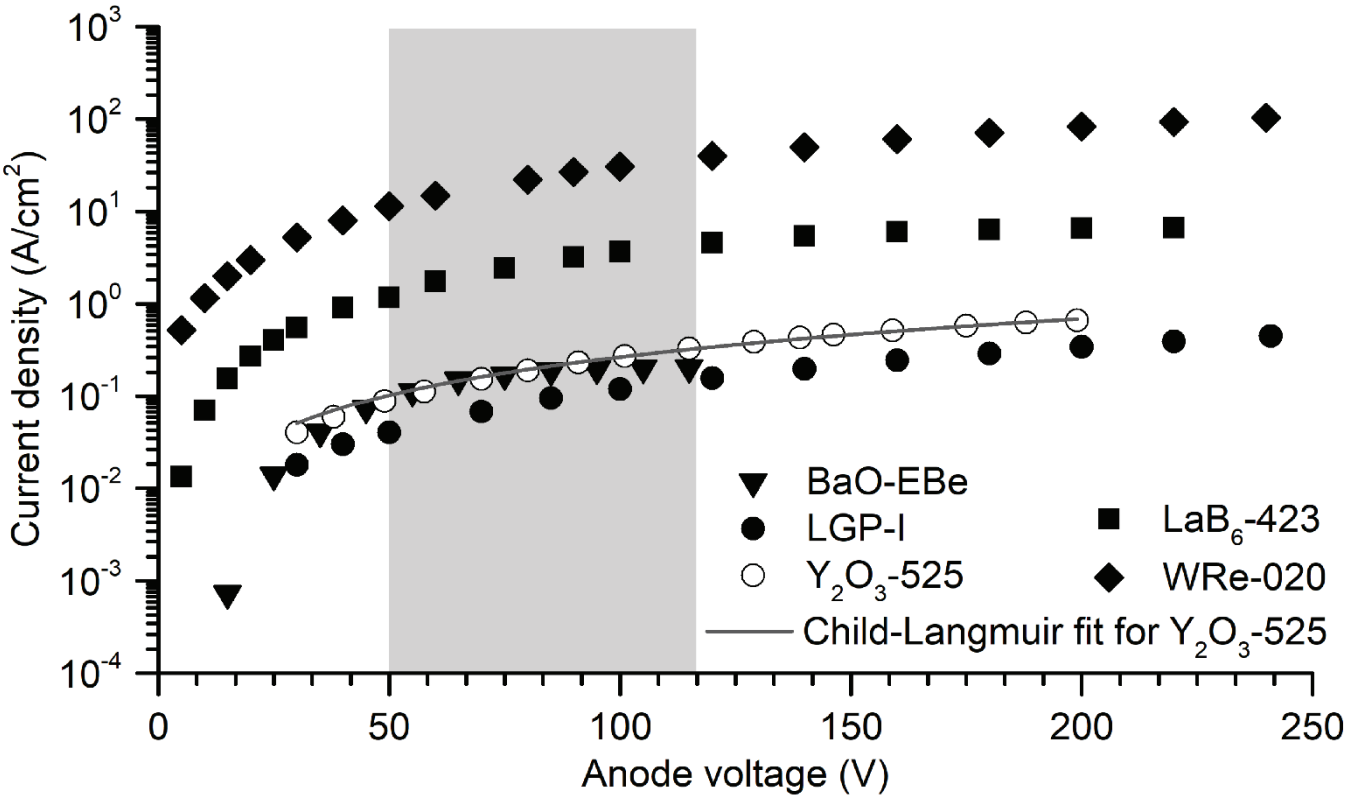

Figure 4. Increasing the anode voltage in a diode setup causes a transition from the space charge limited region at low anode voltages to a temperature limited region, as described by the Child-Langmuir law. The nominal integral acceleration voltage equals 70 V to benefit from the maximal ionization cross section in the range between about 50 and 120 eV (grey).

4. Selection of the Cathodes

Since the launch of ROSETTA in 2004, we have been evaluating cathodes to further improve their performance and anticipate space qualification for likely upcoming missions. Wherever possible, we used them for prototyping and our laboratory instruments as well.

Cathodes for STROFIO / BepiColombo

The selection process for STROFIO illustrated that the choice of the cathode includes accepting many trade-offs, but the achievable power consumption dominated the choice. The WRe-020 hairpin filament consumed about 2.8 W for the desired anode current of 1 mA and a moderate lifetime was expected. The single-crystal lanthanum hexaboride LaB_6-423 cathode is considered a reliable and stable cathode. Tests performed at our institute showed that a lifetime of 2 years with a continuous anode current of 130 µA can be expected [23]. Also, the filament survived vibration tests. However, it consumed almost 4 W for the desired anode current, which was unacceptable.

In contrast, the CNT-XIN carbon nanotubes are supposed to operate with lower power. However, given the coarse grid, one needs to apply high voltages, exceeding 1400 V. In hindsight, the coarse grid was responsible for the poor electron extraction efficiency. We resumed the concept years later for a pressure gauge, and for a potential use in miniaturized mass spectrometers. Optimizing the geometry provides indeed better results [73], [74]. However, even for the newest generations of carbon nanotubes [75], we observed lifetimes well below 1000 hours. Besides the actual lifetime of the CNTs, a parasitic coating of the spacers separating the extraction grid from the substrate where the CNTs are grown on remains a challenge. We found carbon tracks on some of the devices, causing shorts. As neither the lifetime nor the reliability requirements have been fulfilled, we have discarded the idea of using carbon nanotubes several times, which aligns with similar investigations by others (e.g., reference [76]).

Figure 4 indicates current densities of tested cathodes. Especially the BaO-EBe, also referred to as E-Beam, and the LGP-I cathodes were considered more promising. BaO-EBe achieved the shown emission characteristics at 0.7 W, as indicated by the manufacturer. Barium oxide cathodes require complex activation procedures once exposed to air upon operation, ideally temperature controlled [77]. It was also unclear at that time how much the lifetime of the filament would be compromised by frequent air exposure during its early life. In addition, cathode production was discontinued, leading to too many risks for the project. A similar cathode was still available, BaO-EBe. Despite having a similarly complex activation procedure due to the barium oxide, it

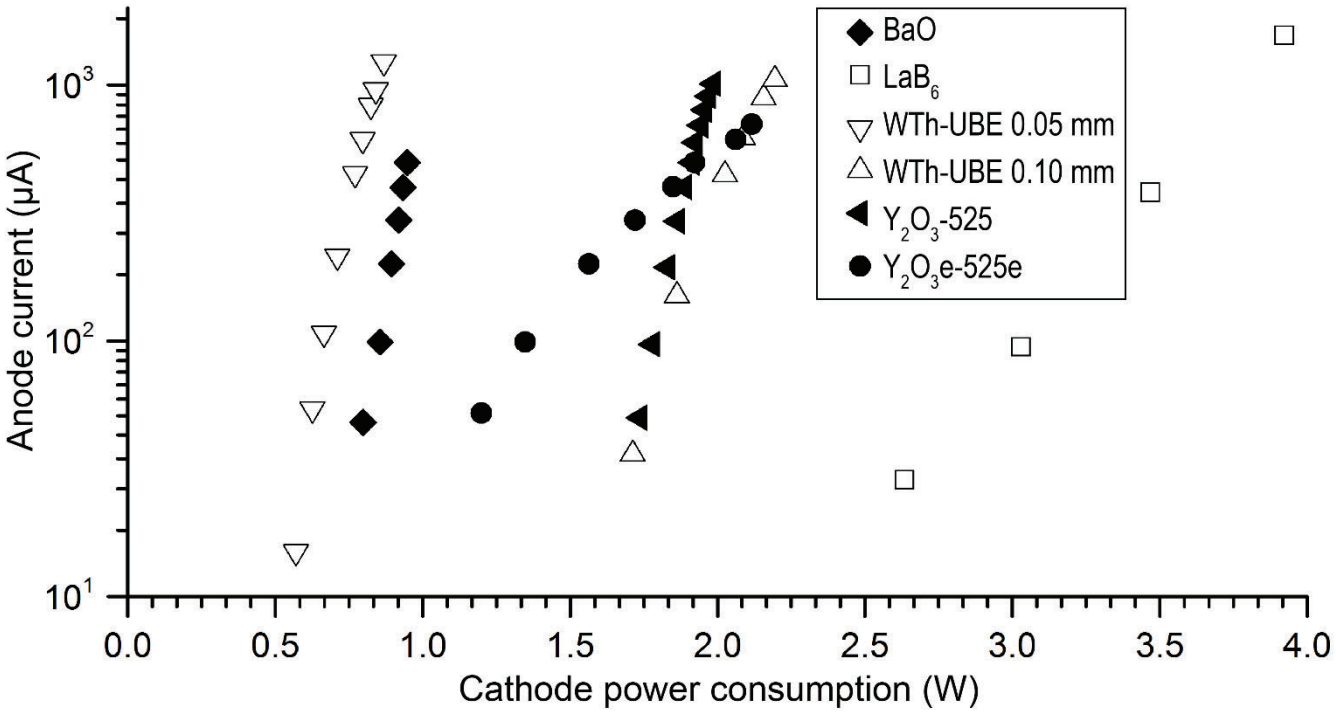

Figure 5. Anode current of cathodes tested in the diode setup (open markers) and ion source mockup (filled markers).

provided 1 mA anode current at a power consumption below 2 W. In fact, the anode current varied between from about 0.65 W at the beginning to about 1.8 W towards end of life. The initial life test, which included two venting cycles, showed that it operated for about 140 days.

Given the alternatives, the BaO-EBe cathode was selected. As the cathode was sensitive to air exposure, the process of selecting the very flight cathode from the batch of purchased cathodes was challenging. Despite the manufacturer's clear warning about performance degradation of the cathode due to repeated venting cycles, the team determined it was necessary to conduct a functional verification before employing it in a flight instrument. Post-use verification with microscopes led to the final selection of the flight cathode.

Y_2O_3-525 was already considered at that time, but we decided that further investigation is necessary before using it for spaceflight, postponing its candidacy for the next instrument.

Cathodes for NGMS / Luna 27

The selection of the cathodes for NGMS implemented lessons learned from STROFIO, especially with respect to activation procedures. Figure 5 shows the power consumption of some cathodes tested. Initial tests of the WTh-UBE cathodes were promising. We were able to use a wire containing 15% Th to form a hairpin filament, considerably lowering the power consumption, which was well below 1 W. However, its expected lifetime and especially its radioactivity discouraged us from further considering the cathode.

We continued testing the Y_2O_3-525 cathode. Its performance is also shown in Figure 5, indicating a power consumption just below 2 W. In parallel, tests with the NGMS ion source were conducted, resulting in a newer upper limit of the anode current of 600 µA with a nominal value of 200 µA, relieving the search for cathodes thanks to the temperature relation indicated in Equation (4). In contrast to the hairpin emitter, this disk emitter provided a bigger surface for emission, allowing for a moderate current density while achieving the requested anode current (Figure 4). Using Equation (3), the Child-Langmuir fit leads to the numeric values of the parameters $\alpha = (4.7 \pm 0.6) \cdot 10^{-4}$ and $k = 1.38 \pm 0.03$ ($R^2 = 0.998$). The distance in the diode setup remained constant in these tests but the current density would vary quadratically in such a case. Hence, there is a high sensitivity towards the position of the filament with respect to the electrodes of the electron optical system.

A benefit for this Y_2O_3 disk emitter is its immunity towards venting cycles with respect to the overall lifetime. During nominal life tests, we performed several venting cycles. The activation procedure of this cathode is simple and can easily be transferred into software reliably. Figure 6 shows the life test of three Y_2O_3-525 cathodes for space qualification. For this test, we purged the system with particle-filtered air instead of dry nitrogen to ensure contamination with air (e.g., oxygen and water). The tests showed a short increase of power consumption upon exposure to air, exponentially decaying with a time constant of about 77 h. We found lifetimes exceeding 8,000 h and concluded a nominal lifetime of about 5,000 to 6,000 hours, aligning with the manufacturer's specification. In addition, the cathode passed shock and vibration testing. Given these advantages, we

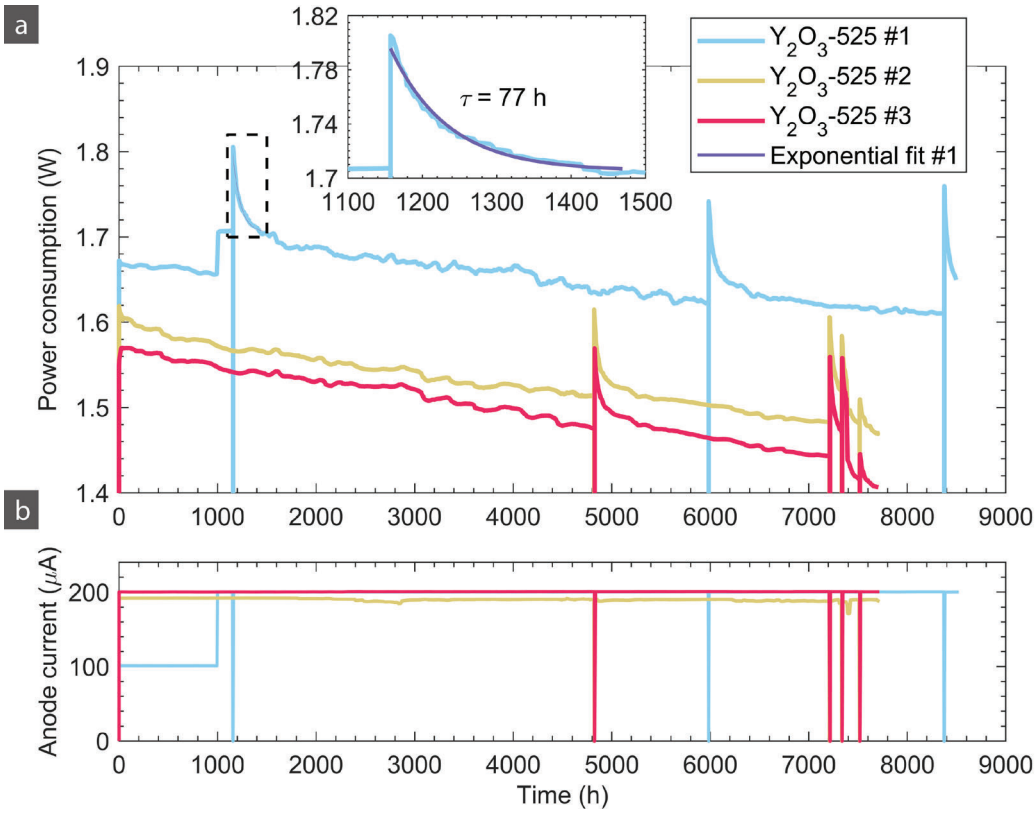

Figure 6. Overview of the lifetime test of three cathodes of type Y_2O_3 (orange, blue, red) in a diode configuration. The power consumption of all cathodes decreased over time (a). The zoom in panel (a) shows a an exponentially decreasing power consumption with a characteristic time constant τ upon air-expsoure to air (dark blue), attributed to outgassing. Anode current of the cathodes during testing (b). An anode current of 0 µA indicates a purging of the system for both inspection and maintainance.

selected this cathode to be the flight cathode for the NGMS instrument. Yet, we typically operate the NGMS proto flight model (PFM) at 1.6 W and the flight spare instrument (FS) at about 1.8 W.

Cathodes for NIM / JUICE

The ion source of NIM shares its basic cathodes configuration with NGMS. Despite originally only anode current of 300 µA were requested; providing them over the required lifetime of 10,000 hours while consuming about 1 W is a challenge. As the development of NIM was initiated at the time of NGMS, all cathodes discussed so far were considered. Noteworthy is the re-consideration of the LaB_6-423 cathode thanks to its outstanding emission stability. However, we dismissed it due to its high-power consumption.

In contrast, the manufacturer of the power-efficient BaO-EBe cathode specified a high lifetime of about 50,000 h if venting was omitted. However, despite it initially operating at a low power consumption, we measured a considerable increase at end of life, as discussed before. In terms of mission planning, this was considered unacceptable because the spacecraft will have to operate in the Jovian system with reduced resources at the end of the mission. Hence, we tested another barium oxide cathode, BaO-015. It showed reasonable emission performance (see Figure 5). Less sensitive to air exposure, but still too much, the activation procedure persisted to be challenging for implementation in the flight software (e.g., reference [56] and references therein). We used advanced surface analysis techniques, including backscattered electron and secondary electron modes with scanning electron microscopes, to justify this assumption. For example, Figure 7 shows the surface of a cathode suffering from overcurrent during early testing. The disk of the cathode becomes visible because the coating evaporated unexpectedly fast. During a life test including repeated both ON/OFF and venting cycling, some analyzed cathodes showed end of life sooner than expected. During testing, on one hand, we observed a lifetime of up to 2100 h including 9 venting cycles with related subsequent activation. On the other hand, four out of five cathodes tested in the mockup setup achieved a lifetime of about 2600 h with 6 venting cycles and 327 ON/OFF cycles, at a power consumption well below 1 W [71].

We found that no suitable cathode possessing at least a moderate technical readiness level for the JUICE mission was available on the market.

Thanks to the team's experience with MCPs and spaceborne high voltage power supplies the development of an MCP-Beam was straightforward. We developed a device and tested it in the diode setup, but with the internal electron-optical

system of the cathode. Unfortunately, the efficiency of the system was below its expectations, mostly due to the low intensity of the available 255 nm LEDs. In addition, the lifetime of the MCPs directly depends on their radiation environment. With about 1.5 mm of Ta shielding, a gain suppression of a factor of 100 would be achieved, and a lifetime of about 6,000 h was estimated. This contrasts with the MCPs inside the detector, which last longer, as less charge is deposited on them, and which is shielded better [7]. Despite this promising concept would even allow for a 360° field of view of NIM, we dropped the concept as well.

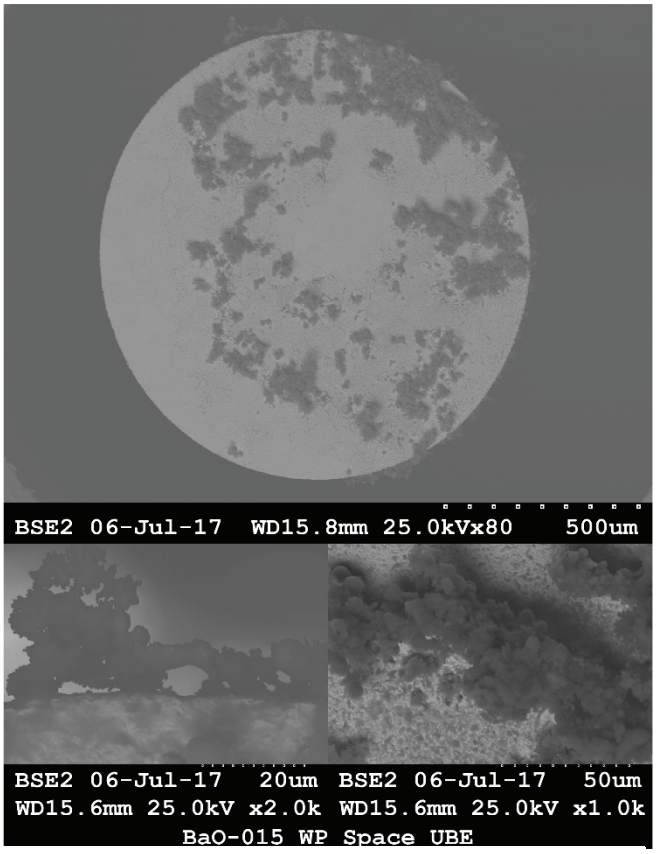

Figure 7. The disc of the BaO-015 emitter becomes visible once the coating evaporated.

We collaborated with *Kimball Physics, Wilton, USA* to provide an enhanced version of the Y_2O_3-525 that was successfully tested for NGMS. The manufacturer specified an acceptable power consumption for this Y_2O_3e-525e cathode, in addition to a lifetime of 10,000 hours.

Figure 5 shows the measured power consumption and related anode currents at its first testing in the ion-optical system mockup (see Figure 2, panel d). The power consumption was bigger than expected. Only after further optimization of the electric fields being present the power consumption was about as specified but increasing with age. Two of the tested cathodes shall serve as example: After 2600 h including 327 ON/OFF cycles and 6 venting cycles, the power consumption increased from (1.04 ± 0.03) W to (1.29 ± 0.03) W for the cathode with an anode current of 50 µA and from (1.25 ± 0.04) W to (2.10 ± 0.05) W for the cathode with an anode current of 300 µA. This behavior contrasted with the aging observed in NGMS' Y_2O_3-525 cathode. Investigations attributed the relatively fast increase of the power consumption to geometrical factors of the electron-optical system implying operation in a temperature limited regime, with higher temperatures than simulated for the flight model. Hence, the tests were considered as accelerated tests and discontinued due to the shutdown during the pandemic. As the geometry of the flight version of the electron source slightly differs from the test mockup, the filament is better thermally isolated, and the anticipated operational lifetime on board the spacecraft was reduced due to change in operations, we selected this cathode and performed the necessary environmental tests including shock and vibration.

On the control side, we decided to operate the cathode with AC with a frequency of 30 kHz. In an earlier study, a power saving of around 10% was demonstrated with a comparable cathode [78], [79]. In nominal operation, the cathode current is regulated to a constant anode current. The cathode itself is set to a potential of approximately –70 V to have the electrons with the desired energy available for ionization in the ion source. The cathode itself is surrounded by a repeller electrode with a potential of less than –70 V. A third electrode acts as an acceleration lens. Optimized tuning of all control circuits and the implementation of filtering is essential on the electronic side to achieve stable emission in this AC current controlled configuration.

5. First Results from NIM's Near-Earth Commissioning Phase

Two Y_2O_3e-525e redundant cathodes are implemented in the proto flight instrument (PFM) of NIM. The JUICE spacecraft was successfully launched on April 14, 2023, at 12:14:36 UTC and is now in the cruise phase on its gravity assist trajectory. During the Near-Earth Commissioning Phase (NECP) of JUICE in space, a short time window was allocated for the commissioning of the main cathode on June 2, 2023, afternoon UTC.

Conditioning Procedure

Figure 8 shows the calibrated (according to NASA's science data processing level: 1b) housekeeping of the NIM PFM during NECP during the cathode 1 commissioning window. The controller power, cathode current, and anode current are indicated. Given design optimizations on the circuitry, the NIM PFM controller cannot measure the effective cathode voltage V_c. However, the cathode current is directly monitored. In addition, the instrument monitors the 12 V power supply which supplies various controllers including the cathode controller. As only minor commissioning tasks were ongoing in parallel and most of the subsystems were disabled, the relative change of the power consumption of the 12 V power supply serves as reasonable indicator for the total power consumption of the subsystem. This includes both the cathode itself and its controller, referred to as controller power.

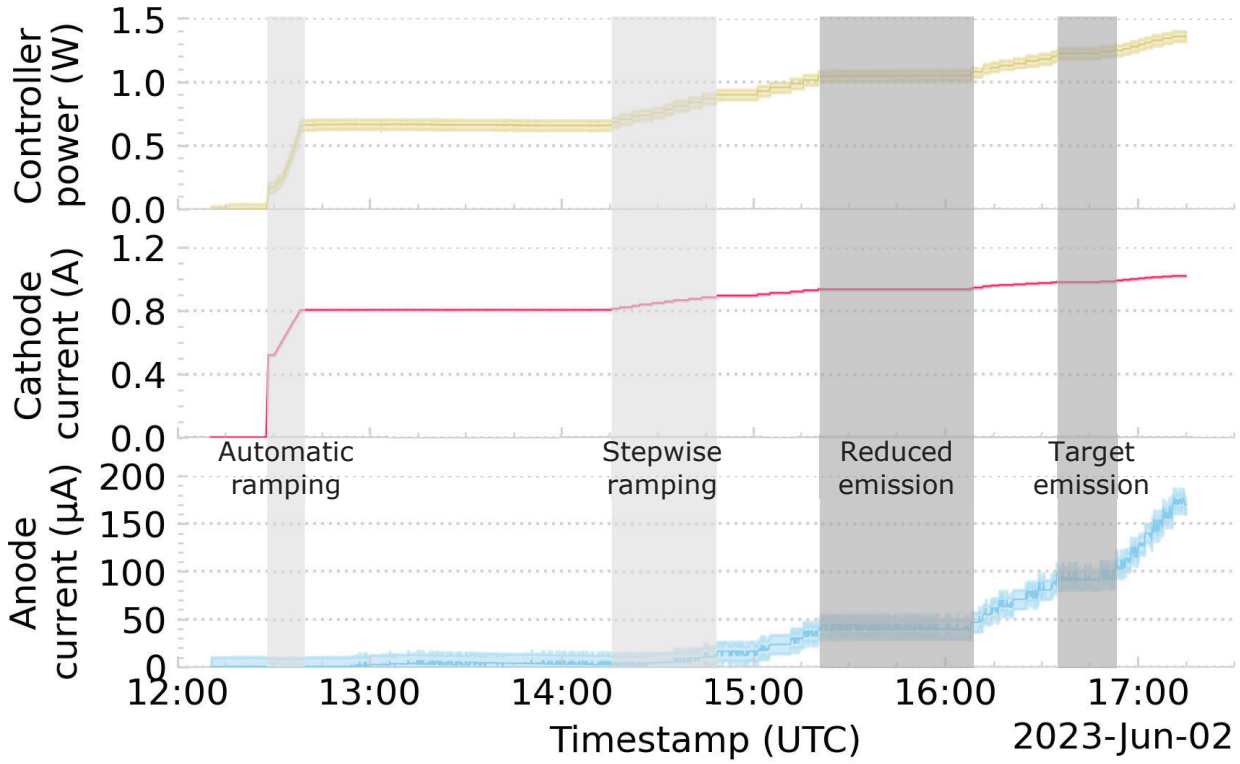

Figure 8. Filament commissioning of NIM PFM during Near-Earth Commissioning Phase. The level 0 data of the 12V power supply indicates the power consumption of the subsystem (see discussion for details, orange). A semi-autonomous increase of the cathode current (red) led to reduced emission at an anode current of 50 µA (blue) and a nominal emission at an anode current of 100 µA, respectively. Light colors indicate error bars.

The aim of this first conditioning was to approach an anode current of at least 100 µA during which the controller operates in open loop. This means that the cathode current was set to a fixed value. Simultaneously, the necessary data for characterizing the cathode were recorded. If the cathode functions as expected, it can then be operated in a closed loop controlled to the desired anode current.

After starting-up of the basic instrument functionalities, the conditioning of the Y_2O_3e-525e cathode 1 was initiated. First the cathode current was automatically ramped to 524 mA with a constant ramp speed of r_I = 780 mA/min. After a pause of 2 min, slower ramping to 806 mA (r_I = 35 mA/min), followed by a break of 97 min was performed. No anode current was detected, as expected. Subsequently, the cathode current was increased by increments of 10 mA. First to 895 mA in 34 min, where an anode current of about 12 µA was observed, then to 937 mA in 19 min and a final anode current of about 40 µA. After another waiting time of 47 min, we continued by steps of 5 mA to 982 mA, where the target anode current of 100 µA occurred the first time. Further increments of the cathode current with same step size to 1019 mA led to an anode current of about 170 µA. The entire conditioning procedure took about 290 minutes. The bias potential was set to –70 V, the entrance slit to 110 V. The repeller, powered by a first quadrant uni-polar power supply, was unregulated which leads to a charging of a few tenth of volts.

The described procedure is of a conservative nature with respect to the waiting times and step sizes. Long waiting times may be due to unexpected operation-specific circumstances (e.g., consultations with cathode specialists) but are not required from a technical point of view. The general procedure for conditioning the redundant cathode is retained. However, an adjustment of the step sizes is discussed, and minimization of the waiting times is intended. Overall, the (almost) real-time interaction between the spacecraft and the ground team operating the instrument was beneficial and recommended for future missions.

The commissioning of cathode 1 up to the upper nominal anode current of 600 µA and of the redundant cathode 2 will be finalized later, when resources become available again.

Flight Cathode Characterization

Figure 9 shows the cathode characteristics of NIM as inferred from the PFM instrument in space and the FS in the laboratory. We show the relationship between cathode current I_c and calculated cathode voltage V_c. Notice the cathode voltage includes the power consumption of the cathode and ohmic losses of the connecting wires. We assume a constant controller efficiency (about 85%), as derived from calibrated calculations. For a cathode current of 1 A, the resistance of the PFM cathode is 0.2 Ohm lower than the one of the FS. As expected, assuming a linearization in the emitting region, the resistances of the hot cathodes can be

described by a constant pseudo resistance R^*: $V_c = (I_c - I_0)R^*$, where I_0 represents an offset. For the PFM, we found $I_{0,PFM} = (0.461 \pm 0.001)$ A and $R^* = (2.4 \pm 0.5)$ Ohm We use this information, together with specifications and preflight characterization of the cathode, to estimate the cathode's temperature for a given cathode current.

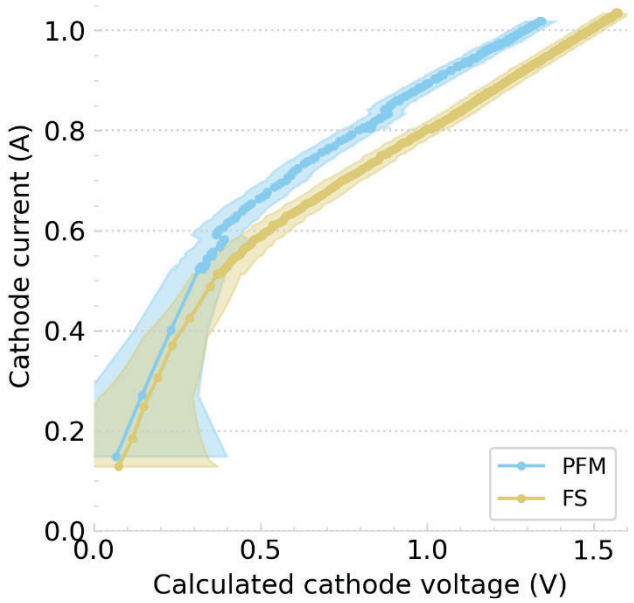

Figure 9. The cathode current as a function of the calculated voltage consumed by the cathode, inferred from calibrated (NASA level: 1b) power measurements. At a cathode current of 1 A, we calculated a resistance of (1.29 ± 0.05) Ohm for the PFM and (1.49 ± 0.05) Ohm for the FS instrument.

Figure 10 shows the measured anode current for an applied cathode current during the conditioning and the fit using Equation (4). The Richardson constant A_G is kept free while the work function Φ was constrained between 2.4 and 2.6 eV, the expected range for this cathode. The hereby found Richardson constant is about seven times lower than expected. However, this result is consistent with the general observation that the cathode current for a desired anode current in flight is higher than for the same cathode in the laboratory. For an anode current of (170 ± 10) µA, the cathode current was 0.95 A in the laboratory and (1.02 ± 0.01) A during flight, respectively. A detailed investigation is ongoing.

It is noteworthy that the temperatures on board the spacecraft, especially the temperature of the ion source and the card rack (housing the electronics and data processing unit) influence the power consumption. Additionally, the instrument supply voltage and the momentary FPGA resource consumption due to parallel processes considerably influence the presented calibrated housekeeping data as well. Further assessment of the modifications in the extraction voltage to reproduce Child-Langmuir's law would be helpful to estimate the

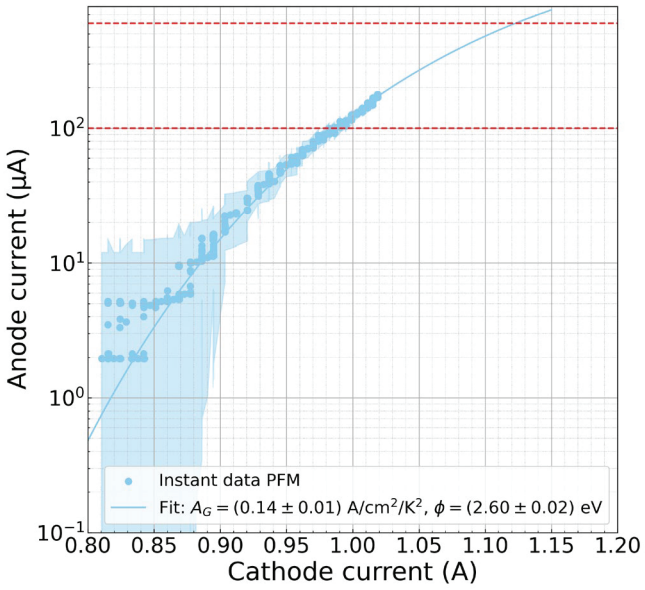

Figure 10. Measured and calibrated anode current for a given cathode current during the conditioning of the PFM cathode, assessed in space. The Richardson Equation (4) is fitted to the data by using prior characterization knowledge of the cathode, manufacturer specifications and the cathode voltage inferred of the total power consumption. The red, dashed line indicates the operational regime.

operation regime with respect to temperature, i.e., to better estimate its expected lifetime. Consequently, further investigation of the data with both the proto flight model and the flight spare model is needed before being able to reliably estimate operation parameters. However, the initial test demonstrated a technical readiness level of 9 of the Y_2O_3e-525e cathode, showing good performance.

6. Re-Flight of the NIM Cathode and Cathodes for Rapid Prototyping

Other instruments in the institute's pipeline will make use of the NIM Y_2O_3e-525e cathode namely CubeSatTOF / CHESS [30] and the sensor head unit (SHU, mass spectrometer) and the neutral density gauge (NDG) of MANIaC / Comet Interceptor [69] . Therefore, we need to carefully understand the cathode's operation parameters in space, ideally over the complete parameter space. Inquiries with the manufacturer indicated no supply issues soon.

Given the performance and the availability of the NGMS Y_2O_3-525 cathode, we used it for laboratory instruments and rapid prototyping, including the MEFISTO-TOF instrument for analyzing gas released from irradiated ice samples [71]. However, the cathode was recently replaced by a successor device due to shortage of supply material. Fortunately, the Y_2O_3W-535W cathode provides similar characteristics, in fact even lower power consumption, and we were able implement this device on several instruments.

The MCP-Beam concept was limited by the intensity of the available UV-LEDs at that time. Thanks to technological advancements, more powerful LEDs are commercially available nowadays. A removal of the high-voltage pulser would compensate for the increased power consumption. The pulser providing 600 V in about 3 ns risetime as a start signal [78], inserting the ions into the mass analyzer, becomes obsolete as the start signal is initiated by triggering the LED using this cathode. Besides a pulsed ionization would be a considerable simplification of the electronics, about 1.6 W of the pulser [78] could be reallocated. Hence, the power consumption of the LED could be increased considerably. The trade-off would be, however, that the storage factor indicated in Equation (1) becomes s = 1, hence, the ion source would lose it storage capabilities.

Even after about 20 years of technological advancements in vacuum electronics, the Spindt type cathodes are still considered the best of class for cold emitters for spaceborne mass spectrometers – but unavailable. Recently, there has been some interest in chasing these developments. For example, Liu et al. [80] discussed opportunities in modern microtips arrays. Despite providing a low technical readiness level, the method is promising to sustainably replace the oxide cathodes, which were invented more than 120 years ago [16] but are still the best of class with respect to handling, power consumption and lifetime and are actually available.

7. Conclusion

Our comprehensive examination of several types of electron emitters aimed to identify options that offer low power consumption and a significant lifespan, ranging between approximately 1000 to 10,000 hours. These emitters were evaluated for their robustness to endure handling and the rigorous conditions of space launch. Our motivation stemmed from the imperative to transition from the traditional WRe emitters, facilitating enhanced power efficiency that could unlock new mission possibilities, including explorations of Mercury, Moon, and Jupiter. Our findings affirm the continued relevance of hot cathodes. However, we replaced the WRe emitters with oxide cathodes. These advanced cathodes exhibit a lifetime of about 10,000 hours, with a modest power consumption of around 1 W, delivering an anode current between 50 to 300 µA. We have qualified such cathodes for space and demonstrated an operation by the successful commissioning of an oxide cathode in NIM on board JUICE, attaining a technical readiness level of 9. This innovation in cathode technology is poised to be a cornerstone for future mass spectrometers, prominently featuring in missions like CubeSatTOF / CHESS and MANIaC / Comet Interceptor.

Appendix

A. Manufacturer of Cathodes

E-Beam Inc., 21070 SW Tile Flat Rd, Beaverton, Oregon, USA.

LG-Philips, does not exist anymore.

Kimball Physics Inc., 311 Kimball Hill Rd, Wilton, NH 03086, USA.

Photonis USA Inc., PO Box 1159, Sturbridge, Massachusetts, USA.

LED Engin Inc., 651 River Oaks Parkway, San Jose, California, USA.

LG Innotek Co. Ltd., 30, Magokjungang 10-ro, Gangseo-gu, Seoul, Republic of Korea.

Xintek Inc., 7020 Kit Creek Road, Suite 200, Research Triangle Park, North Carolina, USA.

List of Abbreviations, Acronyms, and Symbols

AC	Alternating Current
BSE	BackScattered Electron mode
CHESS	Constellation of High-performance Exospheric Science Satellites
CLPS	Commercial Lunar Payload Service
CNT	Carbon Nanotube
COPS	COmet Pressure Sensor
COSAC	COmetary Sampling And Composition
CRT	Cathode Ray Tubes
CubeSatTOF	CubeSat Time-Of-Flight mass spectrometer
DFMS	Double Focusing Mass Spectrometer
EDX	Energy Dispersive X-ray mode
EM	Engineering Model
EQM	Engineering Qualification Model
FN	Fowler–Nordheim
FPGA	Field Programmable Gate Array
FS	Flight Spare model
GCMS	Gas Chromatograph Mass Spectrometer
GPIMS	Galileo Probe Mass Spectrometer
INMS	Ion and Neutral Mass Spectrometer
JUICE	JUpiter ICy moon Explorer
LACE	Lunar Atmospheric Composition Experiment
LADEE	Lunar Atmosphere and Dust Environment Explorer
LED	Light-Emitting Diode
LV	Low Voltage
MANIaC	Mass Analyzer for Neutrals and Ions at Comets
MASPEX	MAss Spectrometer for Planetary EXploration
MAVEN	Mars Express, Venus Express, and Mars Atmosphere and Volatile Evolution
MCP	Multi-Channel Plate
MEFISTO	MEsskammer für FlugzeitInStrumente und Time-Of-Flight (Measurement chamber for TOF instruments)
MEFISTO-TOF	MEFISTO-Time-Of-Flight instrument
MENCA	Mars Exospheric Neutral Composition Analyser
MOMA	Mars Organic Molecule Analyser
MSL	Mars Science Laboratory
MSOLO	Mass Spectrometer Observing Lunar Operations

NDG	Neutral Density Gauge
NECP	Near-Earth Commissioning Phase
NGIMS	Neutral Gas and Ion Mass Spectrometer
NIM	Neutral and Ion Mass spectrometer
ONMS	Pioneer Venus Orbiter Neutral Mass Spectrometer
PEP	Particle Environment Package
PFM	Proto-Flight Model
QMS	Quadrupole Mass Spectrometer
ROSETTA	Name
ROSINA	Rosetta Orbiter Spectrometer for Ion and Neutral Analysis
RTOF	Reflectron Time-Of-Flight mass spectrometer
SEM	Scanning Electron Microscope
SHU	Sensor Head Unit
SIMION	Commercial software for simulation of trajectories of charged particles
STROFIO	STart from a ROtating FIeld mass spectrOmeter
TBD	To Be Defined
TEGA	Thermal Evolved Gas Analyzer
TOF	Time-Of-Flight
TOF-MS	Time-Of-Flight Mass Spectrometer
UV	UltraViolet
VIS	VISible
A	Area
A_G	Material specific parameter; Richardson constant
d	Anode–cathode gap / distance
e	Elementary charge
I^+	Ion current
I_0	Offset current
I_C	Cathode current
I_e	Electron current
j	Current density
k	Fit parameter
k_B	Boltzmann constant
m	Mass
n_0	Total gas number density
R*	Pseudo resistance
s	Storage factor
T	Absolute temperature
V_C	Cathode voltage
α	Fit parameter
β	Ionization probability
ϵ_0	Space permittivity
σ	Ionization cross section
Φ	Work function

ACKNOWLEDGEMENTS

The financial support by the Swiss National Science Foundation and the Swiss Space Office are gratefully acknowledged. We sincerely thank all staff involved in this activity. The helpful collaboration with industry is acknowledged. We declare no conflict of interests.

REFERENCES

[1] T. D. Mark, "Fundamental aspects of electron impact ionization," *International Journal of Mass Spectrometry and Ion Physics*, vol. 45, no. C, pp. 125–145, Dec. 1982, doi: 10.1016/0020-7381(82)80103-4.

[2] P. J. Linstrom and W. G. Mallard, Eds., *NIST Chemistry WebBook, NIST Standard Reference Database Number 69*, vol. 69. Gaithersburg MD: National Institute of Standards and Technology, 2023.

[3] H. Balsiger *et al.*, "Rosina – Rosetta Orbiter Spectrometer for Ion and Neutral Analysis," *Space Sci Rev*, vol. 128, no. 1–4, pp. 745–801, May 2007, doi: 10.1007/s11214-006-8335-3.

[4] S. Gasc, "Sensitivity and Fragmentation Calibration of the ROSINA Reflectron-type Time-Of-Flight Mass Spectrometer," PhD Thesis, University of Bern, 2015.

[5] D. Abplanalp, "Development of a sensitive TOF-Mass Spectrometer for Space Research," PhD Thesis, University of Bern, 2009.

[6] D. Abplanalp, P. Wurz, L. Huber, and I. Leya, "An optimised compact electron impact ion storage source for a time-of-flight mass spectrometer," *Int J Mass Spectrom*, vol. 294, no. 1, pp. 33–39, Jun. 2010, doi: 10.1016/j.ijms.2010.05.001.

[7] M. Föhn, A. Galli, A. Vorburger, M. Tulej, D. Lasi, A. Riedo, R. G. Fausch, M. Althaus, S. Brungger, P. Fahrer, M. Gerber, M. Luthi, H. P. Munz, S. Oeschger, D. Piazza, and P. Wurz, "Description of the Mass Spectrometer for the Jupiter Icy Moons Explorer Mission," *2021 IEEE Aerospace Conference*, pp. 1–14, Mar. 2021, doi: 10.1109/AERO50100.2021.9438344.

[8] R. Grix, U. Grüner, G. Li, H. Stroh, and H. Wollnik, "An electron impact storage ion source for time-of-flight mass spectrometers," *Int J Mass Spectrom Ion Process*, vol. 93, no. 3, pp. 323–330, Oct. 1989, doi: 10.1016/0168-1176(89)80121-1.

[9] C. D. Child, "Discharge From Hot CaO," *Physical Review (Series I)*, vol. 32, no. 5, pp. 492–511, May 1911, doi: 10.1103/PhysRevSeriesI.32.492.

[10] I. Langmuir, "The Effect of Space Charge and Residual Gases on Thermionic Currents in High Vacuum," *Physical Review*, vol. 2, no. 6, pp. 450–486, Dec. 1913, doi: 10.1103/PhysRev.2.450.

[11] J. H. Hoffman, R. R. Jr. Hodges, F. S. Johnson, and D. E. Evans, "Lunar orbital mass spectrometer experiment," 1973.

[12] R. G. Fausch, J. A. Schertenleib, and P. Wurz, "Advances in Mass Spectrometers for Flyby Space Missions for the Analysis of Biosignatures and Other Complex Molecules," *Universe*, vol. 8, no. 8, p. 416, Aug. 2022, doi: 10.3390/universe8080416.

[13] O. W. Richardson, "The Emission of Electrons from Tungsten at High Temperatures: An Experimental Proof That the Electric Current in Metals Is Carried by Electrons," *Science (1979)*, vol. 38, no. 967, pp. 57–61, Jul. 1913, doi: 10.1126/science.38.967.57.

[14] O. W. Richardson, "On the Negative Radiation from Hot Platinum," *University Press*, 1901.

[15] R. Jenkins, "A review of thermionic cathodes," *Vacuum*, vol. 19, no. 8, pp. 353–359, Jan. 1969, doi: 10.1016/S0042-207X(69)80077-1.

[16] G. Gaertner and D. den Engelsen, "Hundred years anniversary of the oxide cathode—A historical review," *Appl Surf Sci*, vol. 251, no. 1–4, pp. 24–30, Sep. 2005, doi: 10.1016/j.apsusc.2005.03.214.

[17] G. Gaertner, "Historical development and future trends of vacuum electronics," *Journal of Vacuum Science & Technology B, Nanotechnology and Microelectronics: Materials, Processing, Measurement, and Phenomena*, vol. 30, no. 6, p. 060801, 2012, doi: 10.1116/1.4747705.

[18] D. den Engelsen and G. Gaertner, "Rare earth oxide doping in oxide cathodes," *Appl Surf Sci*, vol. 253, no. 2, pp. 1023–1028, 2006, doi: 10.1016/j.apsusc.2006.04.046.

[19] A. Bhardwaj, S. V. Mohankumar, T. P. Das, P. Pradeepkumar, P. Sreelatha, B. Sundar, A. Nandi, D. P. Vajja, M. B. Dhanya, N. Naik, G. Supriya, R. Satheesh Thampi, G. Padma Padmanabhan, V. K. Yadav, and A. V. Aliyas, "MENCA experiment aboard India's Mars Orbiter Mission," *Curr Sci*, vol. 109, no. 6, pp. 1106–1113, 2015, doi: 10.18520/cs/v109/i6/1106-1113.

[20] A. Vorburger, P. Wurz, and H. Waite, "Chemical and Isotopic Composition Measurements on Atmospheric Probes Exploring Uranus and Neptune," *Space Sci Rev*, vol. 216, no. 4, 2020, doi: 10.1007/s11214-020-00684-9.

[21] R. S. Gurnee, S. Livi, M. L. Phillips, M. I. Desai, J. R. Hayes, G. C. Ho, R. Hourani, S. Jaskulek, and J. Scheer, "Strofio: A novel neutral mass spectrograph for sampling Mercury's exosphere," *IEEE Aerospace Conference Proceedings*, 2012, doi: 10.1109/AERO.2012.6187066.

[22] S. Orsini, S. Livi, K. Torkar, S. Barabash, A. Milillo, P. Wurz, A. M. Di Lellis, and E. Kallio, "SERENA: A suite of four instruments (ELENA, STROFIO, PICAM and MIPA) on board BepiColombo-MPO for particle detection in the Hermean environment," *Planet Space Sci*, vol. 58, no. 1–2, pp. 166–181, Jan. 2010, doi: 10.1016/j.pss.2008.09.012.

[23] P. Wahlström, "Development of Instrumentation for the experimental investigation of Mercury' s Atmosphere," PhD Thesis, University of Bern, 2011.

[24] V. G. Istomin, K. V. Grechnev, and V. A. Kotchnev, "Mass Spectrometer Measurements of the Composition of the Lower Atmosphere of Venus," in *COSPAR Colloquia Series*, vol. 20, no. C, COSPAR, 1980, pp. 215–218. doi: 10.1016/S0964-2749(13)60044-X.

[25] H. B. Niemann, J. R. Booth, J. E. Cooley, R. E. Hartle, W. T. Kasprzak, N. W. Spencer, S. H. Way, D. M. Hunten, and G. R. Carignan, "Pioneer Venus Orbiter Neutral Gas Mass Spectrometer Experiment," *IEEE Transactions on Geoscience and Remote Sensing*, vol. GE-18, no. 1, pp. 60–65, 1980, doi: 10.1109/TGRS.1980.350282.

[26] L. Colin and D. M. Hunten, "11. Pioneer venus experiment descriptions," *Space Sci Rev*, vol. 20, no. 4, pp. 451–525, Jul. 1977, doi: 10.1007/BF02186463.

[27] M. Rodriguez, N. Paschalidis, S. Jones, E. Sittler, D. Chornay, P. Uribe, T. Cameron, and B. Nanan, "A Compact Ion and Neutral Mass Spectrometer for CubeSat/SmallSat Platforms," in *Proceedings of the 29th Small Satellite Conference*, Logan, UT, USA, 2015. [Online]. Available: https://digitalcommons.usu.edu/smallsat/2015/all2015/103/

[28] L. Kepko, L. Santos, C. Clagett, B. Azimi, D. Chai, A. Cudmore, S. Starin, J. Marshall, and J. Lucas, "Dellingr: Reliability lessons learned from on-orbit," *Proceedings of the Small Satellite Conference*, vol. SSC18-I–01, 2018, [Online]. Available: https://digitalcommons.usu.edu/cgi/viewcontent.cgi?article=4062&context=smallsat

[29] N. P. Paschalidis, S. L. Jones, M. Rodriguez, P. Uribe, T. Cameron, J. Dennis, E. Sittler, and A. Glocer, "Initial Results from the mini Ion and Neutral mass Spectrometer on the NSF Exocube and NASA Dellingr missions .," in *EPSC-DPS2019*, 2019. [Online]. Available: https://meetingorganizer.copernicus.org/EPSC-DPS2019/EPSC-DPS2019-1885-1.pdf

[30] R. G. Fausch, C. Zimmermann, T. Gerber, J. Schertenleib, M. Föhn, A. E. Aebi, and P. Wurz, "Monitoring Space Weather with a Sensitive 1 U CubeSat Mass Spectrometer," *2023 IEEE Aerospace Conference*, pp. 1–11, Mar. 2023, doi: 10.1109/AERO55745.2023.10115572.

[31] R. C. Elphic and C. T. Russell, *The Lunar Atmosphere and Dust Environment Explorer Mission (LADEE)*. Cham: Springer International Publishing, 2015. doi: 10.1007/978-3-319-18717-4.

[32] B. A. Cohen, S. J. Barber, W. M. Farrell, A. D. Morse, S. Sheridan, N. M. Curran, M. Leese, C. Howe, P. Driggers, and R. Trautner, "The peregrine ion trap mass spectrometer (PITMS): A CLPS-delivered ion trap mass spectrometer for in-situ studies of the lunar water cycle," in *51nd Lunar and Planetary Science Conference 2020*, 2020, pp. 1–2. [Online]. Available: https://www.hou.usra.edu/meetings/lpsc2020/pdf/1091.pdf

[33] R. A. Ayala, M. L. Hancock, A. W. Jarnot, J. E. Captain, and J. W. Quinn, "Mass Spectrometer Observing Lunar Operations (MSolo)," in *71st ASMS Conference on Mass Spectrometry and Allied Topics*, Huston, Texas, Jun. 2023. Accessed: Oct. 01, 2023. [Online]. Available: https://ntrs.nasa.gov/citations/20230007808

[34] D. R. Rushneck, A. V. Diaz, D. W. Howarth, J. Rampacek, K. W. Olson, W. D. Dencker, P. Smith, L. McDavid, A. Tomassian, M. Harris, K. Bulota, K. Biemann, A. L. LaFleur, J. E. Biller, and T. Owen, "Viking gas chromatograph–mass spectrometer," *Review of Scientific Instruments*, vol. 49, no. 6, pp. 817–834, Jun. 1978, doi: 10.1063/1.1135623.

[35] D. M. Anderson, K. Biemann, L. E. Orgel, J. Oro, T. Owen, G. P. Shulman, P. Toulmin, and H. C. Urey, "Mass spectrometric analysis of organic compounds, water and volatile constituents in the atmosphere and surface of Mars: The Viking Mars Lander," *Icarus*, vol. 16, no. 1, pp. 111–138, Feb. 1972, doi: 10.1016/0019-1035(72)90140-6.

[36] J. H. Hoffman, R. C. Chaney, and H. Hammack, "Phoenix Mars Mission-The Thermal Evolved Gas Analyzer," *J Am Soc Mass Spectrom*, vol. 19, no. 10, pp. 1377–1383, 2008, doi: 10.1016/j.jasms.2008.07.015.

[37] P. R. Mahaffy *et al.*, "The sample analysis at mars investigation and instrument suite," *Space Sci Rev*, vol. 170, no. 1–4, pp. 401–478, 2012, doi: 10.1007/s11214-012-9879-z.

[38] P. R. Mahaffy *et al.*, "The Neutral Gas and Ion Mass Spectrometer on the Mars Atmosphere and Volatile Evolution Mission," *Space Sci Rev*, vol. 195, no. 1–4, pp. 49–73, Dec. 2015, doi: 10.1007/s11214-014-0091-1.

[39] W. B. Brinckerhoff, V. T. Pinnick, F. H. W. Van Amerom, R. M. Danell, R. D. Arevalo, M. S. Atanassova, X. Li, P. R. Mahaffy, R. J. Cotter, F. Goesmann, and H. Steininger, "Mars Organic Molecule Analyzer (MOMA) mass spectrometer for ExoMars 2018 and beyond," *IEEE Aerospace Conference Proceedings*, pp. 1–8, 2013, doi: 10.1109/AERO.2013.6496942.

[40] R. Arevalo, W. Brinckerhoff, F. Van Amerom, R. Danell, V. Pinnick, X. Li, S. Getty, L. Hovmand, A. Grubisic, P. Mahaffy, F. Goesmann, and H. Steininger, "Design and demonstration of the Mars Organic Molecule Analyzer (MOMA) on the ExoMars 2018 rover," *IEEE Aerospace Conference Proceedings*, vol. 2015-June, pp. 1–11, 2015, doi: 10.1109/AERO.2015.7119073.

[41] H. B. Niemann, D. N. Harpold, S. K. Atreya, G. R. Carignan, D. M. Hunten, and T. C. Owen, "Galileo Probe Mass Spectrometer experiment," *Space Sci Rev*, vol. 60, no. 1–4, pp. 111–142, May 1992, doi: 10.1007/BF00216852.

[42] M. Föhn, "NIM: The Neutral Gas and Ion Mass Spectrometer to Explore the Galilean Ice Worlds," PhD Thesis, University of Bern, 2021. [Online]. Available: https://boristheses.unibe.ch/id/eprint/3277

[43] M. Hässig, M. Libardoni, K. Mandt, G. Miller, and R. Blase, "Performance evaluation of a prototype multi-bounce time-of-flight mass spectrometer in linear mode and applications in space science," *Planet Space Sci*, vol. 117, pp. 436–443, 2015, doi: 10.1016/j.pss.2015.09.006.

[44] W. Kasprzak, H. Niemann, D. Harpold, J. Richards, H. Manning, E. Patrick, and P. Mahaffy, "Cassini orbiter ion and neutral mass spectrometer instrument," *Proc SPIE Int Soc Opt Eng*, vol. 2803, no. Cassini/Huygens: A Mission to the Saturnian Systems, pp. 129–140, 1996, doi: 10.1117/12.253413.

[45] H. B. Niemann *et al.*, "The gas chromatograph mass spectrometer for the Huygens probe," *Space Sci Rev*, vol. 104, no. 7, pp. 553–591, 2002, doi: https://doi.org/10.1023/A:1023680305259.

[46] F. Goesmann, S. McKenna-Lawlor, R. Roll, J. H. Bredehöft, U. Meierhenrich, F. Raulin, W. Thiemann, G. M. Muñoz Caro, and C. Szopa, "Interpretation of COSAC mass spectrometer data acquired during Rosetta's Lutetia fly-by 10 July 2010," *Planet Space Sci*, vol. 66, no. 1, pp. 187–191, 2012, doi: 10.1016/j.pss.2012.01.012.

[47] F. Goesmann, H. Rosenbauer, R. Roll, C. Szopa, F. Raulin, R. Sternberg, G. Israel, U. Meierhenrich, W. Thiemann, and G. Munoz-Caro, "Cosac, The Cometary Sampling and Composition Experiment on Philae," *Space Sci Rev*, vol. 128, no. 1–4, pp. 257–280, May 2007, doi: 10.1007/s11214-006-9000-6.

[48] Shults, "ROSETTA - A comet rendezvous mission," in *1st international workshop for landing site selection for Russian Moon Lander "Luna-Glob,"* Moscow, Russia: IKI Space Research Institute, Moscow, Russia, 2011. [Online]. Available: http://iki.cosmos.ru/conf/2011-lg/presentations/2_DAY/

[49] J. F. J. Todd, S. J. Barber, I. P. Wright, G. H. Morgan, A. D. Morse, S. Sheridan, M. R. Leese, J. Maynard, S. T. Evans, C. T. Pillinger, D. L. Drummond, S. C. Heys, S. E. Huq, B. J. Kent, E. C. Sawyer, M. S. Whalley, and N. R. Waltham, "Ion trap mass spectrometry on a comet nucleus: the Ptolemy instrument and the Rosetta space mission," *Journal of Mass Spectrometry*, vol. 42, no. 1, pp. 1–10, Jan. 2007, doi: 10.1002/jms.1147.

[50] G. Gaertner, D. Raasch, D. Barratt, and S. Jenkins, "Accelerated life tests of CRT oxide cathodes," *Appl Surf Sci*, vol. 215, no. 1–4, pp. 72–77, 2003, doi: 10.1016/S0169-4332(03)00282-4.

[51] J.-Y. Gao, Y.-F. Yang, X.-K. Zhang, S.-L. Li, P. Hu, and J.-S. Wang, "A review on recent progress of thermionic cathode," *Tungsten*, vol. 2, no. 3, pp. 289–300, 2020, doi: 10.1007/s42864-020-00059-1.

[52] P. Wurz, D. Abplanalp, M. Tulej, and H. Lammer, "A neutral gas mass spectrometer for the investigation of lunar volatiles," *Planet Space Sci*, vol. 74, no. 1, pp. 264–269, 2012, doi: 10.1016/j.pss.2012.05.016.

[53] G. Gaertner and D. Barratt, "Life-limiting mechanisms in Ba-oxide, Ba-dispenser and Ba-Scandale cathodes," *Appl Surf Sci*, vol. 251, no. 1–4, pp. 73–79, 2005, doi: 10.1016/j.apsusc.2005.03.213.

[54] D. S. Barratt and S. N. Jenkins, "The evolution of oxide cathodes for cathode ray tube applications," *Journal of Materials Science: Materials in Electronics*, vol. 17, no. 9, pp. 735–743, 2006, doi: 10.1007/s10854-006-0020-5.

[55] D. S. Barratt, N. Filkin, and I. Bakker, "12.3: Oxide Plus - A Newly Developed Cathode for CRT Applications," *SID Symposium Digest of Technical Papers*, vol. 34, no. 1, p. 162, 2003, doi: 10.1889/1.1832229.

[56] G. Gärtner and P. A. M. van der Heide, "New Developments in CRT Cathodes," in *IDW 2000, Kobe, Japan, Technical Digest CRT4--1*, Kobe, Japan, 2000, pp. 513–516.

[57] S. Tsujino, P. Beaud, E. Kirk, T. Vogel, H. Sehr, J. Gobrecht, and A. Wrulich, "Ultrafast electron emission from metallic nanotip arrays induced by near infrared femtosecond laser pulses," *Appl Phys Lett*, vol. 92, no. 19, May 2008, doi: 10.1063/1.2924290.

[58] P. Helfenstein, E. Kirk, K. Jefimovs, T. Vogel, C. Escher, H.-W. Fink, and S. Tsujino, "Highly collimated electron beams from double-gate field emitter arrays with large collimation gate apertures," *Appl Phys Lett*, vol. 98, no. 6, Feb. 2011, doi: 10.1063/1.3551541.

[59] C. A. Spindt, C. E. Holland, A. Rosengreen, and I. Brodie, "Field-Emitter Arrays for Vacuum Microelectronics," *IEEE Trans Electron Devices*, vol. 38, no. 10, pp. 2355–2363, 1991, doi: 10.1109/16.88525.

[60] R. Baptist, "Bayard–Alpert vacuum gauge with microtips," *Journal of Vacuum Science & Technology B: Microelectronics and Nanometer Structures*, vol. 14, no. 3, p. 2119, May 1996, doi: 10.1116/1.588883.

[61] J. D. Levine, "Benefits of the lateral resistor in a field effect display," *Journal of Vacuum Science & Technology B: Microelectronics and Nanometer Structures*, vol. 14, no. 3, p. 2008, May 1996, doi: 10.1116/1.588975.

[62] D. Temple, "Recent progress in field emitter array development for high performance applications," *Materials Science and Engineering: R: Reports*, vol. 24, no. 5, pp. 185–239, Jan. 1999, doi: 10.1016/S0927-796X(98)00014-X.

[63] M. Rubin, K. Altwegg, A. Jäckel, and H. Balsiger, "Development of a low energy ion source for ROSINA ion mode calibration," *Review of Scientific Instruments*, vol. 77, no. 10, p. 103302, Oct. 2006, doi: 10.1063/1.2358708.

[64] J. Schiedt and R. Weinkauf, "Efficient and robust anion source, based on a microchannel plate electron source," *Review of Scientific Instruments*, vol. 70, no. 5, pp. 2277–2281, 1999, doi: 10.1063/1.1149752.

[65] H. S. Kim, S. Y. Kim, and M. Yang, "Cold electron source with an electron multiplier illuminated by ultraviolet photons," *Anal Chem*, vol. 84, no. 8, pp. 3635–3639, Apr. 2012, doi: 10.1021/ac203486u.

[66] W. Jeong, H. S. Kim, and B. Kang, "Development of a portable time-of-flight mass spectrometer prototype using a cold electron source," *Review of Scientific Instruments*, vol. 93, no. 2, Feb. 2022, doi: 10.1063/5.0074883.

[67] D. Abplanalp, P. Wurz, L. Huber, I. Leya, E. Kopp, U. Rohner, M. Wieser, L. Kalla, and S. Barabash, "A neutral gas mass spectrometer to measure the chemical composition of the stratosphere," *Advances in Space Research*, vol. 44, no. 7, pp. 870–878, Oct. 2009, doi: 10.1016/j.asr.2009.06.016.

[68] L. Hofer, P. Wurz, A. Buch, M. Cabane, P. Coll, D. Coscia, M. Gerasimov, D. Lasi, A. Sapgir, C. Szopa, and M. Tulej, "Prototype of the gas chromatograph–mass spectrometer to investigate volatile species in the lunar soil for the Luna-Resurs mission," *Planet Space Sci*, vol. 111, no. 1, pp. 126–133, Jun. 2015, doi: 10.1016/j.pss.2015.03.027.

[69] C. Snodgrass and G. H. Jones, "The European Space Agency's Comet Interceptor lies in wait," *Nat Commun*, vol. 10, no. 1, pp. 1–4, 2019, doi: 10.1038/s41467-019-13470-1.

[70] L. Hofer, "Development of the gas chromatograph – mass spectrometer to investigate volatile species in the lunar soil for the Luna-Resurs mission," PhD Thesis, University of Bern, 2015.

[71] R. G. Fausch, "Mass Spectrometry for In Situ Planetary Research," PhD Thesis, University of Bern, Switzerland, 2020. doi: 10.7892/boris.144755.

[72] S. Meyer, "Development of a Neutral Gas- and Ion-Mass Spectrometer for Jupiter' s Moons," PhD Thesis, University of Bern, 2017.

[73] H. Zhang, D. Li, P. Wurz, R. G. Fausch, Z. Ma, J. Ge, and Y. Yin, "A Study of Collimated Electron Source for Highly Stable Ionisation Gauge," *IEEE 10th International Workshop on Metrology for AeroSpace (MetroAeroSpace)*, pp. 1–5, Jun. 2023.

[74] Z. Ma, D. Li, H. Zhang, P. Wurz, R. G. Fausch, Y. Cheng, P. Yao, J. Ge, X. Han, G. Li, Y. Wang, and C. Dong, "Study of a low-energy collimated beam electron source and its application in a stable ionisation gauge," *Vacuum*, vol. 215, no. 6, p. 112302, Sep. 2023, doi: 10.1016/j.vacuum.2023.112302.

[75] H. Zhang, D. Li, P. Wurz, Y. Cheng, Y. Wang, C. Wang, J. Sun, G. Li, and R. G. Fausch, "Residual Gas Adsorption and Desorption in the Field Emission of Titanium-Coated Carbon Nanotubes," *Materials*, vol. 12, no. 18, pp. 2937–2949, Sep. 2019, doi: 10.3390/ma12182937.

[76] S. A. Getty, L. F. Lim, A. Grubisic, A. E. Southard, J. Ferrance, M. A. Balvin, X. Li, T. Cornish, J. Elsila, L. A. Hess, C. A. Kotecki, J. G. Hagopian, and W. B. Brinckerhoff, "Future planetary instrument capabilities made possible by micro- and nanotechnology," in *Micro- and Nanotechnology Sensors, Systems, and Applications XI*, M. S. Islam and T. George, Eds., SPIE, May 2019, p. 14. doi: 10.1117/12.2519455.

[77] G. Gaertner, "Modern Developments in Ba Oxide Cathodes," in *Modern Developments in Vacuum Electron Sources. Topics in Applied Physics*, vol. 135, G. Gaertner, W. Knapp, and R. G. Forbes, Eds., in Topics in Applied Physics, vol. 135. , Cham: Springer International Publishing, 2020, pp. 173–219. doi: 10.1007/978-3-030-47291-7_4.

[78] R. G. Fausch, P. Wurz, M. Tulej, J. Jost, P. Gubler, M. Gruber, D. Lasi, C. Zimmermann, and T. Gerber, "Flight electronics of GC-mass spectrometer for investigation of volatiles in the lunar regolith," *2018 IEEE Aerospace Conference*, pp. 1–13, 2018, doi: 10.1109/AERO.2018.8396788.

[79] D. Lasi, S. Meyer, D. Piazza, M. Luthi, A. Nentwig, M. Gruber, S. Brungger, M. Gerber, S. Braccini, M. Tulej, M. Fohn, and P. Wurz, "Decisions and Trade-Offs in the Design of a Mass Spectrometer for Jupiter's Icy Moons," in *2020 IEEE Aerospace Conference*, IEEE, Mar. 2020, pp. 1–20. doi: 10.1109/AERO47225.2020.9172784.

[80] W. Liu, X. Zhang, H. Liu, J. Li, N. Zhou, Y. Liu, and Q. Lu, "Field emission and electron beam transmission characteristics of microtips array on the (100) plane of

single-crystal Gadolinium hexaboride ceramic," *Ceram Int*, vol. 48, no. 6, pp. 8395–8402, Mar. 2022, doi: 10.1016/j.ceramint.2021.12.046.

BIOGRAPHY

Rico G. Fausch *completed an apprenticeship as a mechanical design engineer before he received a B.Sc. in Systems Engineering (micro technologies) from NTB University of Applied Science (Switzerland) in 2013 and an M.Sc. in Biomedical Engineering from University of Bern (Switzerland) in 2015. He has been with the Physics Institute of the University of Bern since 2016, where he received his Ph.D. in Physics in 2020 for the finalization of the NGMS / Luna 27. As an instrument scientist, he is involved in the design of several space missions and space instrumentation including NIM / PEP / JUICE (ESA) and CODEX / DIMPLE / CLPS (NASA).*

Martina Föhn *received an M.Sc. in physics from the University of Bern in 2017, with a thesis on the scattering properties of charge state conversion surfaces for space applications for the JUICE and the IMAP missions. She has received a Ph.D. in physics in 2021 for the development of the flight instrument of NIM and its calibration.*

Lukas Hofer *received an M.Sc. in physics from the University of Bern in 2011, and a Ph.D. in 2015 for the development of the NGMS instrument on board the Luna 27 mission. He is now CTO and Co-founder at a startup, where he is responsible for the development of commercial mass spectrometers.*

Stefan Meyer *received an M.Sc. in physics from the University of Bern in 2013, and a Ph.D. in 2017 for the development of the prototype instrument of NIM on board JUICE. After a postdoc at the University hospital in Bern, Switzerland, he moved to industry as a systems engineer and project lead.*

Peter Wahlström *received an M.Sc. in physics from the University of Bern in 2006, and a Ph.D. in 2011 for his contributions to the STROFIO instrument on board BepiColombo. He moved to industry, where he develops software solutions.*

Samuel S. Wyler *received an M.Sc. in physics from the Ecole polytechnique fédérale de Lausanne (EPFL), Lausanne, Switzerland in 2022. From 2021 to 2022, he specialized in accelerator physics and wrote his Master Thesis in the framework of the AWAKE project at CERN, Geneva, Switzerland. He is pursuing a Ph.D. for the calibration and operation-related scientific activities of NIM / JUICE.*

Peter Wurz *has a degree in electronic engineering (1985), an M.Sc. and a Ph.D. in Physics from Technical University of Vienna, Austria (1990). He has been a post-doctoral researcher at Argonne National Laboratory, USA. Since 1992 at the University of Bern. He is Professor of physics, 2015–2022 head of the Space Science and Planetology division, and since 2022 director of the physics institute. He has been Co-I and PI for many science instruments for space missions of ESA, NASA, ISRO, CNSA, Roscosmos, and JAXA.*